INSTITUTE OF PHYSICS PUBLISHING NANOTECHNOLOGY
Nanotechnology **14** (2003) 670–674 PII: S0957-4484(03)59671-4

Crystallization, phase transition and optical properties of the rare-earth-doped nanophosphors synthesized by chemical deposition

X Y Chen[1], L Yang[2], R E Cook[3], S Skanthakumar[1], D Shi[2] and G K Liu[1,4]

[1] Chemistry Division, Argonne National Laboratory, Argonne, IL 60439, USA
[2] Department of Materials Science and Engineering, University of Cincinnati, Cincinnati, OH 45221, USA
[3] Materials Science Division, Argonne National Laboratory, Argonne, IL 60439, USA

E-mail: gkliu@anl.gov

Received 11 February 2003, in final form 21 March 2003
Published 25 April 2003
Online at stacks.iop.org/Nano/14/670

Abstract
The structural and electronic properties of Eu^{3+}-doped Y_2O_3 films coated on spherical alumina nanoparticles are studied using transmission electron microscope, x-ray diffraction, and laser spectroscopic techniques. It is observed that the coated films crystallize at temperatures higher than 600 °C and may be completely converted into a cubic Y_2O_3 nanocrystalline layer at 750 °C. At 900 °C, phase transition occurs between the outer coating layer and the inner core, and different types of crystalline nanophase can be obtained. In the materials that we prepared and studied, all possible crystallographic phases, including two of solid-state laser media, $YAlO_3$ (YAP), and $Y_3Al_5O_{12}$ (YAG), may be formed in the pseudo-binary Al_2O_3–Y_2O_3 nanosystem by controlling thermal annealing procedures from 600 to 900 °C, a temperature region far below the conventional solid-state reaction temperature. The spectroscopic properties of Eu^{3+} in all the nanophases are characterized in comparison with those of their bulk counterparts.

1. Introduction

Nanocrystalline and nanostructured materials are attracting extensive attention because of their novel electronic, magnetic, optical, or thermal properties in comparison with their bulk counterparts. For rare-earth-doped nanophosphors, several unexpected phenomena have recently been reported. These phenomena include the surface quenching effect [1], modifications in transition intensity and fluorescence lifetime [2], single-ion luminescence [3], restricted phonon relaxation, and anomalous thermalization [4, 5]. Eu^{3+}-doped cubic Y_2O_3 crystals are common red phosphors used in optical display and lighting applications. Nanosized or ultrafine particles of $Eu:Y_2O_3$ prepared by gas-phase condensation or wet chemical methods (e.g. hydrothermal, emulsion, or sol–gel) have been widely studied, including both cubic and monoclinic phases [6, 7]. Few investigations have dealt with layers of phosphors coated on nanoparticles, which, we believe, should exhibit unique nanoscale surface characteristics such as anomalous optical properties and phase transition behaviours.

In this paper we report on the crystallization and phase transition at very low elevated temperatures in a $Eu:Y_2O_3$ layer approximately 10 nm in thickness on alumina nanoparticles, coated using a chemical deposition method (heterogeneous nucleation and growth). The phase transition (Y_2O_3 + $Al_2O_3 \rightarrow YAlO_3$, $Y_3Al_5O_{12}$) across the active surface layer (Y_2O_3) and the core particles (Al_2O_3) occurs near 900 °C, far

[4] Author to whom any correspondence should be addressed.

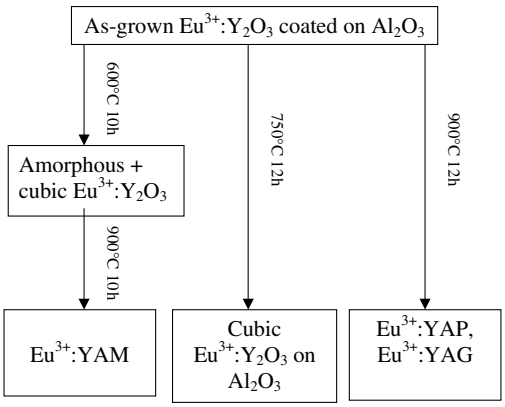

Figure 1. The crystalline phases resulting from thermal annealing of amorphous films of Eu^{3+}:Y_2O_3 coated on Al_2O_3 nanocrystals.

below the conventional solid-state reaction temperature. By means of x-ray diffraction (XRD), transmission electron microscopy (TEM), and laser optical spectroscopy we have observed that the crystalline structures of Y_2O_3, $YAlO_3$ (YAP), $Y_3Al_5O_{12}$ (YAG), and $Y_4Al_2O_9$ (YAM) are formed in the samples annealed at different temperatures. Figure 1 illustrates the temperature-dependent crystallization and phase transition behaviours of the coated nanoparticles. Obviously, the chemical dynamics in the coated nanoparticles are rather complex, and the thermodynamics for bulk systems is not applicable to the nanoscale systems. Given that the single crystals of YAP and YAG are important laser hosts, and usually grown from the melt by the Czochralski technique at high temperature (>1800 °C), studies of the nanodynamics of crystal growth may help in developing new techniques in materials sciences.

2. Synthesis method

The samples were prepared by heterogeneous chemical deposition as follows. The starting spherical gamma-Al_2O_3 nanoparticles were purchased from Nanophase Ltd. The particle size ranges between 27 and 56 nm, with a specific surface area of 30–60 $m^2\ g^{-1}$. A total of 0.5 g of particles were dispersed in 300 ml of deionized water and ultrasonically vibrated for 0.5 h. After stabilization for 30 min, the solution was divided into equal portions and certain amounts of YCl_3 (0.2 mol l^{-1}) and $EuCl_3$ (0.2 mol l^{-1}) were added. For the sample studied in this research, the Al:Y:Eu ratio was kept at 100:40:1. While being sonically vibrated, the solution was titrated with ammonia (1 mol l^{-1}) at speed of 10 ml/10 min. Just before the pH reached the isoelectric point of yttria, i.e., slightly above 8, both vibration and titration were stopped to allow incubation for more than 2 h. The process was then continued to fully deposit the Y^{3+}. The precipitates were separated and collected by centrifuging and rinsing, then dried and ground. The temperature of the drying process was strictly controlled: changed at a rate of 20 °C h^{-1} from 30 to 300 °C, held at 300 °C for 3 h, and finally lowered to room temperature at a rate of 50 °C h^{-1}. To investigate the crystallization and phase transition of the nanocoating phosphors, the as-grown powders were put into several quartz containers and then further annealed in a furnace at 600, 750, and 900 °C, for 12 h. The temperature rose at the intrinsic rate of the furnace. The cooling rate is supposed to be as fast as possible; it was achieved by quenching directly to room temperature in the air within 10 min. The annealing time of 12 h was empirically determined. Shorter time may lead to incomplete crystallization and phase transition, whereas longer time may result in cluster formation and larger particle size.

3. Results and discussion

The XRD, fluorescence spectra, and TEM images of the samples annealed at different temperatures are compared in figures 2–4 respectively. The XRD data were collected from 5° to 150° in a Scintag diffractometer. As shown in figure 2(a), the XRD spectrum of the as-grown sample shows characteristic lines of the Al_2O_3 phase and no evidence of any Y_2O_3 phase, which indicates that the coating layers of Y_2O_3 are amorphous in nature and most of them are actually in the form of yttrium oxyhydroxide (YOOH). As reported by Rao [6], the conversion of yttrium oxyhydroxide to oxide (or the crystallization) started at a temperature of 562 °C for ultrafine Y_2O_3 particles prepared by sol–gel methods. Similarly, drying below 300 °C during the preparation of the as-grown nanocoating samples can only get rid of the adsorbed water molecules, and not chemically bonded water. The XRD spectrum of the sample annealed at 600 °C, figure 2(b), shows clearly the intermediate phases between the crystalline and amorphous phases. It contains a large amount of amorphous phase of the alumina matrix, and small amounts of cubic Y_2O_3 and Y_3O_4Cl crystalline phases. The impurity phase of Y_3O_4Cl could be formed accidentally during the co-deposition processes; it no longer exists in the 750 °C annealed sample. These results indicate that the layers of Eu:Y_2O_3 coated on Al_2O_3 particles using chemical deposition have nearly the same crystallization temperature as the particles prepared by the sol–gel method [6]. When the as-grown sample is heated at 750 °C for 12 h, the crystallization is almost complete. As shown in figure 2(c), the XRD spectra show an exclusive cubic Y_2O_3 crystal phase except for some residuals of the alumina particles.

More curiously, when the as-grown sample was annealed at 900 °C, not only did crystallization occur but also new phases were formed due to efficient transportation of the Eu:Y_2O_3 and Al_2O_3 phases across the interfaces between the coated layer and the core particle. As shown in figure 2(d), approximately 62% of YAP, 38% of cubic YAG, and residual Al_2O_3 phases are identified in analysis of the XRD spectrum of the 900 °C annealed samples. When the as-grown sample was annealed at the same temperature by a step-by-step procedure (600 °C for 10 h, then 900 °C for 10 h), as shown in figure 2(e), another possible crystalline structure in the Y_2O_3–Al_2O_3 system: monoclinic $Y_4Al_2O_9$ (YAM) nanocrystal, was observed as the dominant component of the final product.

The crystallization behaviours and nanophase transitions have been studied in more detail in our laser spectroscopic experiments. For recording the time-resolved fluorescence spectra, a pulsed dye laser with a tunable range from 510 to 550 nm, or an ultraviolet (UV) pulsed laser at 355 nm, was used to pump the samples. The dye laser wavelength was tuned to excite the $^7F_0 \rightarrow {}^5D_1$ transition in Eu^{3+} as a probe of crystalline lattices surrounding the Eu^{3+} ions. The fluorescence of Eu^{3+} ($^5D_0 \rightarrow {}^7F_0$, $^7F_1$, and $^7F_2$) in the range of 570–640 nm was recorded, and the decay time of the Eu^{3+} fluorescence was

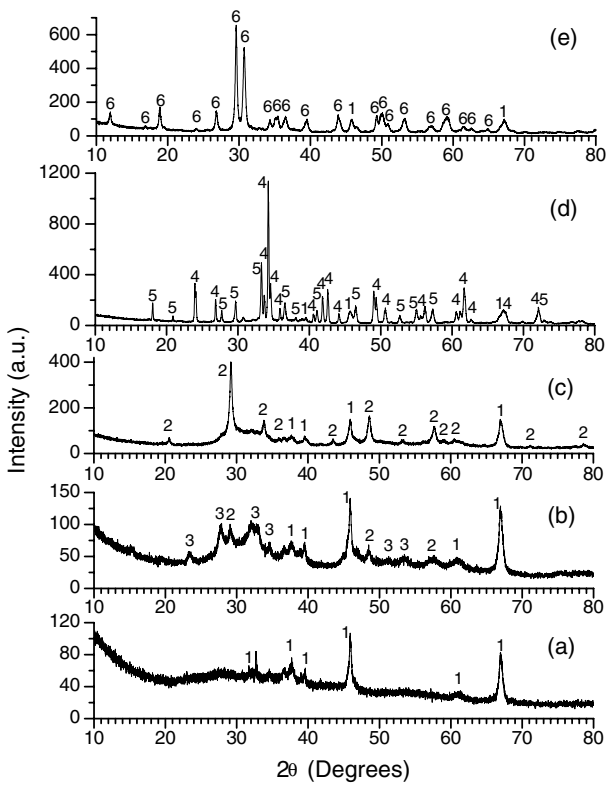

Figure 2. XRD spectra of (a) the sample as-grown; (b) the sample annealed at 600 °C; (c) the sample annealed at 750 °C; (d) the sample annealed at 900 °C; (e) the sample annealed step by step (600 → 900 °C). All the phases are well identified according to the standard data published by the International Centre for Diffraction Data (ICDD). (a) Al_2O_3 (No 77-0396); (b) Al_2O_3 (No 77-0396) + Y_2O_3 (No 74-0553) + Y_3O_4Cl (No 21-1451); (c) Y_2O_3 (No 74-0553) + Al_2O_3 (No 77-0396); (d) YAP (No 70-1677) + YAG (No 79-1891) + Al_2O_3 (No 77-0396); (e) YAM(No 34-0368) + Al_2O_3 (No 77-0396). The values in the above parentheses are ICDD numbers. All phases are listed in the order of decreasing intensity. Lines marked by numbers 1, 2, 3, 4, 5, and 6 in the figure correspond respectively to Al_2O_3, Y_2O_3, Y_3O_4Cl, YAP, YAG and YAM crystalline phases.

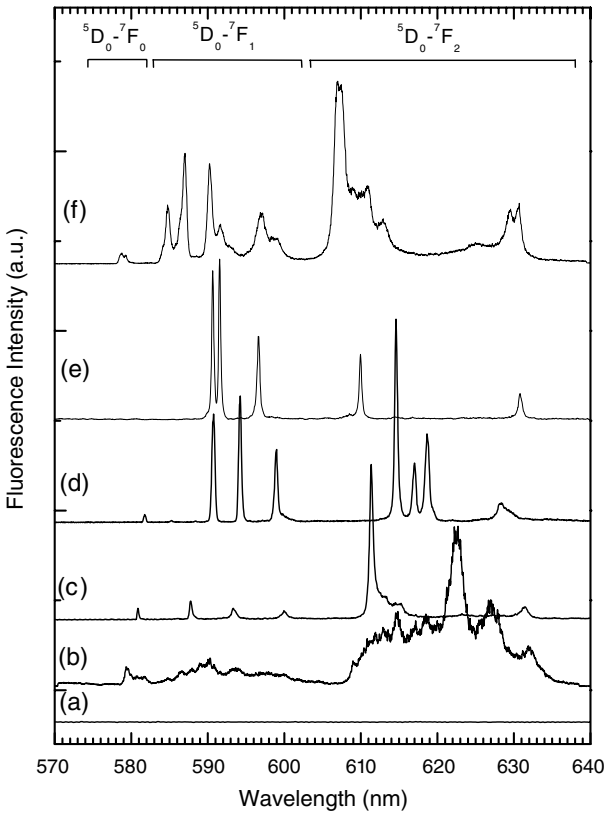

Figure 3. Emission spectra of (a) the Eu^{3+}:Y_2O_3/Al_2O_3 sample as grown, $\lambda_{exc} = 355$ nm; (b) the sample annealed at 600 °C, $\lambda_{exc} = 526.98$ nm; (c) the sample annealed at 750 °C (Eu^{3+}:Y_2O_3), $\lambda_{exc} = 528.09$ nm; (d) the sample annealed at 900 °C (Eu^{3+}:YAP), $\lambda_{exc} = 528.43$ nm; (e) the sample annealed at 900 °C (Eu^{3+}:YAG), $\lambda_{exc} = 527.60$ nm; (f) the sample annealed step by step (600 → 900 °C, Eu^{3+}:YAM), $\lambda_{exc} = 526.61$ nm. All spectra were recorded at 3.5 K. The fluorescence emission was detected using a boxcar integrator that averaged the fluorescence signal from a cooled PMT with 15 μs gate and 0.3 ms delay from the pump laser pulse.

measured using a digital storage oscilloscope. As shown in figure 3, no Eu^{3+} fluorescence lines are recorded for the as-grown sample, possibly due to non-radiative quenching by surface defects. For the sample annealed at 600 °C, however, the Eu^{3+} fluorescence lines are observed, but the linewidth is much broader than that of Eu^{3+} in a crystalline phase, thus suggesting that the Eu^{3+} ions have amorphous environments. In contrast, the narrow peaks in the emission spectrum of the samples annealed at 750 °C (figure 3(c)) are from the fluorescence of Eu^{3+} ions in a crystalline lattice. The structure of the spectrum with energy levels in good agreement with the previous works [8] suggests a site of C_2 symmetry in the cubic Y_2O_3 crystal. For the samples annealed at 900 °C, the spectrum shows that Eu^{3+} ions occupy two different lattice sites (YAP and YAG), which have been separately detected using site-selected laser excitation. When the laser was tuned to excite the Eu^{3+} ions ($^7F_0 \rightarrow {}^5D_1$, 528.43 nm) in the YAP lattice (figure 3(d)), only single sites of Eu^{3+} in YAP crystal were found. Although currently no additional data on the crystal-field levels of Eu^{3+}:YAP are available for an exclusive site assignment, the positions of the first four emission lines ($^5D_0 \rightarrow {}^7F_0$, $^7F_1$) are coincident with a previous report on these energy levels of Eu^{3+}:YAP [9]. When the laser was tuned to excite the Eu^{3+} ions ($^7F_0 \rightarrow {}^5D_1$, 527.60 nm) in the YAG lattice (figure 3(e)), it excited simultaneously some Eu^{3+} ions at the YAP site due to the coincident overlap of the excitation peak of Eu^{3+}:YAP at 527.93 nm. Therefore the emission spectrum (figure 3(e)) consists of contributions overwhelmingly from the Eu^{3+}:YAG site and weakly from the minor Eu:YAP site. The emission lines originating from Eu^{3+} sites in the YAG lattice match well with the previously reported energy levels [10]. As for the sample annealed in two steps (600 and 900 °C, held for 10 h each), the emission spectrum at 3.5 K, as shown in figure 3(f), indicates that Eu^{3+} ions occupy at least three different sites in the YAM lattice. Due to the low spectral resolution at room temperature, Liu *et al* [11] reported only two kinds of Eu^{3+} site. The results of optical spectroscopic experiments independently identify the crystalline phases formed from annealing of the coated nanoparticles, thus confirming our XRD findings. Moreover, the spectroscopic results confirm that the each of the crystalline nanophases contains Eu^{3+} ions as luminescence centres.

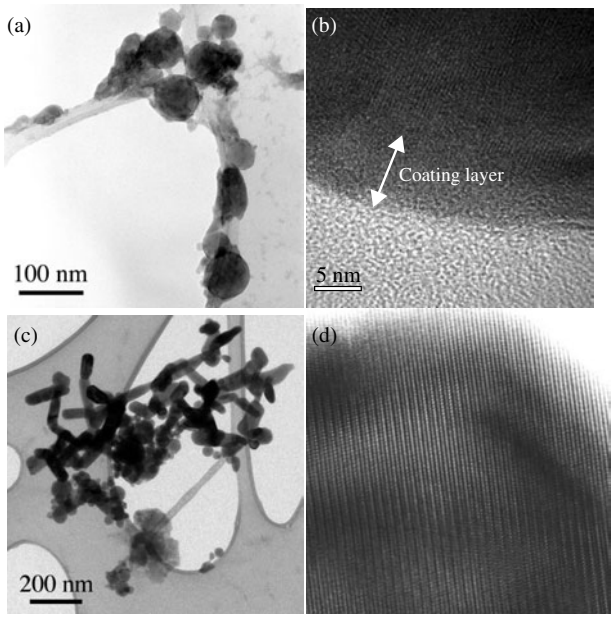

Figure 4. (a) A TEM image of the as-grown sample: alumina nanoparticles coated with Eu^{3+}:Y_2O_3; (b) a high-resolution TEM image of the coating layer in a selected Eu^{3+}:Y_2O_3/Al_2O_3 nanoparticle (as grown); (c) a TEM image of the sample annealed at 900 °C for 12 h; (d) a high-resolution TEM image of an individual nanoparticle in the sample annealed at 900 °C, showing the atomic lattice alignment.

The fluorescence lifetimes of Eu^{3+} ions in the coated and annealed nanocrystals have been measured at liquid helium and room temperatures respectively, and are listed in table 1. Because direct measurement of the lifetime of $^5D_1$ at room temperature is difficult, the lifetime at room temperature is determined according to the initial rising edge of the $^5D_0$ decay curves [12]. All the decay curves from $^5D_0$ fit well to a single exponential, indicating no energy transfer. This is different from the case of coating on micro-alumina cores [13]. At 3.5 K, the lifetime of $^5D_0$ in the phase of cubic Y_2O_3 (1.43 ms) is found to be unusually longer than the longest value of the bulk counterparts ever reported (1.1 ms) [14], whereas the $^5D_1$ lifetime (∼68 μs) is much shorter than the reported values (90–120 μs). The longer lifetime of $^5D_0$ in the Eu:Y_2O_3 nanolayer is most probably due to the non-solid medium surrounding the nanoparticles that changes the effective index of refraction, thus changing the radiative lifetime [2]. The filling factor, showing what fraction of space is occupied by the nanoparticles, is estimated to be approximately 84% according to equation (1) of [2], where the index of refraction of the surrounding medium (helium gas) and that of cubic Y_2O_3 are assumed to be 1.0 and 1.915, respectively, for the gas and the nanoparticles. The same occurs to the lifetime of $^5D_0$ in the YAP phase. It is observed that the lifetime of $^5D_0$ in YAP at 3.5 K (1.64 ms) is larger than Weber's value (1.5 ms) [12], which corresponds to a filling factor of ∼94%, but the $^5D_1$ lifetime (45 μs) is much shorter than the reported 65 μs in spite of the lower temperature in our experiment. The lifetimes of $^5D_0$ and $^5D_1$ in YAG agree well with Gross's report [15]. The lifetimes of Eu^{3+} in YAM are reported for the first time in the present work. The reason that the $^5D_0$ lifetime in Eu^{3+}:YAM varies significantly with temperature remains unknown. The excited state dynamics might be related to the multi-site structure of the nanocrystals. We also anticipate that, because of the changes in the density of phonon states in the nanostructures, the anomalous dynamics of phonon relaxation in the nanocoating layers may induce the discrepancies in the fluorescence lifetime of the $^5D_1$ state of Eu^{3+} in the nanostructures [5].

Table 1. Fluorescence lifetimes of Eu^{3+} ions in the nanocrystals obtained via the processes of crystallization and phase transition of the same batch of coated nanophosphors. (Values in parentheses are experimental temperatures.)

	Y_2O_3	YAP	YAG	YAM[a]
$^5D_0$ (ms)	1.43 (3.5 K) 1.42 (294 K)	1.64 (3.5 K) 1.37 (294 K)	3.98 (3.5 K) 3.48 (294 K)	4.61 (3.5 K) 3.47 (294 K)
$^5D_1$ (μs)	68 (3.5 K) 13 (294 K)	45 (3.5 K) 28 (294 K)	20 (3.5 K) 11 (294 K)	69 (3.5 K) 21 (294 K)

[a] Lifetimes of the Eu^{3+} at a main site were measured by monitoring the strongest emission at 607.4 nm.

To compare the nanoparticle's morphologies before and after the annealing processes, TEM was performed on a Philips CM30T instrument operated at 200 kV. Figure 4(a) shows the TEM image of the coated alumina nanoparticles, with an average particle size of approximately 60–70 nm. The high-resolution TEM image of a selected nanocrystal (figure 4(b)) shows that the coating layer is approximately 10 nm. The crystalline Al_2O_3 lattice of the core is quite apparent, with the amorphous Y_2O_3 film on the particle surface in accordance with the XRD analyses. The energy-dispersive x-ray spectra also confirm that the coating layer contains Y_2O_3. The TEM images of the annealed samples at 600 and 750 °C show little difference from that of the as-grown sample except for a small modification of the particle morphology due to the crystallization of the nanocoatings. The TEM image of the annealed samples at 900 °C shown in figure 4(c) reveals that most of the nanoparticulate matrix has transformed into elongated particles that are roughly the same size as Al_2O_3 nanospheres. The average size of the cylinder-shape particles is about 110 nm × 50 nm. The crystalline characteristics of the nanoparticles are revealed, as shown in the high-resolution TEM picture of an individual nanocrystal (figure 4(d)).

From the crystallographic point of view, 900 °C is unusually low for enabling the growth of binary crystals in the Y_2O_3–Al_2O_3 system, especially for the form of the YAP crystalline phase. Obviously, the conventional phase diagram of Y_2O_3–Al_2O_3 system, which indicates that bulk YAP melts incongruently and is unstable below 1600 °C [16], is not applicable in the nanoscale thermodynamics. Note that the as-grown nanocoating layers of Eu^{3+}:Y_2O_3 on the core of alumina particles may have extremely high surface energy, which could greatly lower the barrier to the reaction between the core and coating layer. Therefore, it may lead to non-equilibrium phase transition by solid–solid diffusion processes. Generally, the diffusion coefficient D can be expressed as $D = D_0 \exp(-\Delta E/kT)$, where ΔE is the reaction barrier. This barrier is closely related to the lattice binding energy, particle size, and morphology (surface effects). However, a fundamental understanding of the nanoscale chemical reaction and solid–solid diffusion processes has not been achieved yet, and thus needs future studies.

4. Conclusions

In summary, we have observed novel thermodynamic properties of the coated nanoparticles of Eu^{3+}:Y_2O_3/Al_2O_3, prepared by chemical deposition and characterized by XRD, TEM, and laser spectroscopic techniques. The coated layers of Eu^{3+}:Y_2O_3 start crystallization at 600 °C, and completed crystallization can be achieved at 750 °C. Phase transition and formation of binary crystalline phases between the coating layer and the core occur at a temperature (900 °C) far below the transition temperature at which conventional solid-state reaction (1400–1600 °C) occurs in bulk materials. It is interesting that all the possible crystalline phases of the Y_2O_3–Al_2O_3 system can be formed on the basis of the different thermal annealing processes of the as-grown phosphors with the same chemical compositions. By further controlling the composition of the starting materials and the deposition and heating processes, it may be possible to obtain more homogeneous and pure phases of YAP (or YAG) crystalline films coated on the alumina core at lower temperatures, to avoid forming clusters or coalescing.

Acknowledgments

The work at Argonne National Laboratory was performed under the auspices of the Office of Basic Energy Science, Division of Chemical Sciences, the US Department of Energy, under Contract No W-31-109-ENG-38.

References

[1] Tissue B M 1998 *Chem. Mater.* **10** 2837
[2] Meltzer R S, Feofilov S P, Tissue B and Yuan H B 1999 *Phys. Rev.* B **60** R14012
[3] Bartko A P, Peyser L A, Dickson R M, Mehta A, Thundat T, Bhargava R and Barnes M D 2002 *Chem. Phys. Lett.* **358** 459
[4] Meltzer R S and Hong K S 2000 *Phys. Rev.* B **61** 3396
[5] Liu G K, Zhuang H Z and Chen X Y 2002 *Nano Lett.* **2** 535
Liu G K, Chen X Y, Zhuang H Z, Li S and Niedbala R S 2003 *J. Solid State Chem.* at press
[6] Rao R P 1996 *J. Electrochem. Soc.* **143** 189
Rao R P 1996 *Solid State Commun.* **99** 439
[7] Eilers H and Tissue B M 1996 *Chem. Phys. Lett.* **251** 74
Bihari B, Eilers H and Tissue B M 1997 *J. Lumin.* **75** 1
Williams D K, Bihari B, Tissue B M and McHale J M 1998 *J. Phys. Chem.* B **102** 916
[8] Chang N C 1963 *J. Appl. Phys.* **34** 3500
Chang N C and Gruber J B 1964 *J. Chem. Phys.* **41** 3227
[9] Shelby R M and Macfarlane R M 1981 *Phys. Rev. Lett.* **47** 1172
Erickson L E and Sharma K K 1981 *Phys. Rev.* B **24** 3697
Erickson L E 1986 *Phys. Rev.* B **34** 36
[10] Koningstein J A 1964 *Phys. Rev.* **136** A717
Asano M and Koningstein J A 1979 *Chem. Phys.* **42** 369
[11] Liu S and Su Q 1997 *J. Alloys Compounds* **255** 102
[12] Weber M J 1973 *Phys. Rev.* B **8** 54
[13] Gedanken A, Reisfeld R, Sominski L, Zhong Z, Koltypin Yu, Panczer G, Gaft M and Minti H 2000 *Appl. Phys. Lett.* **77** 945
[14] Buijs M, Meijerink A and Blasse G 1987 *J. Lumin.* **37** 9
[15] Gross H, Neukum J, Heber J, Mateika D and Xiao T 1993 *Phys. Rev.* B **48** 9264
[16] Bondar I A, Koroleva L N and Bezruk E T 1984 *Inorg. Mater.* **20** 214